EXPIREMENTAL MEASUREMENT OF THE ELECTRIC NEAR FIELD ON THE BUCK CONVERTER

Abdelhakim Zeghoudi* – Abdelber Bendaoud

Department of Electrical Engineering, Djilali Liabes University, Sidi Bel Abbes, Algeria

ARTICLE INFO

***Article history*:**
Received: 08.01.2025.
Received in revised form: 22.03.2025.
Accepted: 25.03.2025.

Keywords:
Electric Field
Buck converter
Diode
MOSFET
Electronic switching

DOI: https://doi.org/10.30765/er.2776

Abstract:

This paper studies the radiated interference of the near electric field (E-Field) generated by a series chopper, particularly in the main components of the converter: the IR2110 driver, IRF740 MOSFET, and MUR460 diode, using Rohde & Schwarz probes in the frequency domain (FD) by using a spectrum analyzer. The chopper is supplied by a 20 V DC source, and the control signal is a square wave. First, we determine the electrical diagram of converter DC/DC using LTspice software, then implement it on a PCB, in order to quantify the electric field on all the electronic components on all the components. Then the impact of variation the frequency of the commutation the MOSFET was determinated. The following frequencies were used while keeping the duty cycle fixed: 5 kHz, 10 kHz, and 145.3 kHz. Then, we varied the duty cycle, selecting the following values: 75%, 50%, and 25%, while keeping the frequency fixed at 10 kHz. The variation of the series chopper control signal parameters (frequency and duty cycle) is managed by an Arduino program. The results demonstrate that probes with larger surface areas capture a stronger field than those with smaller surface areas. future work, we will study the near magnetic field, and all the parameters that influence magnetic emissions

1 Introduction

DC/DC converters have extensive applications in connecting storage batteries, photovoltaic systems, wind turbines, hybrid systems, and automotive applications. These converters comprise active and passive electronic components [1-4]. With the increasing use of electronic switches controlled at high frequencies, rapid changes in current (di/dt) and voltage (dv/dt) occur, resulting in significant electromagnetic disturbances [5-9]. These disturbances are a part of the electromagnetic compatibility (EMC) issues faced by power converters, affecting their performance and reliability.

A chopper is a DC/DC converter able to convert a fixed DC voltage or current at a given level into a variable DC voltage or current at another level [10].

As shown in Figure 1, a voltage with a variable average value is obtained by periodically connecting and disconnecting the load from the source by means of switches.

Static DC/DC converters consist of active electronic components like such as diodes, MOSFETs, and transistors, as well as passive components such as inductors, capacitors, coupling elements, and parasitic elements. Each of these elements can contribute to electromagnetic disturbances, which can be conducted through cables in common and differential modes or radiated through electromagnetic emissions in the air. These disturbances are inherent to the operation of the converter and can impact the electromagnetic compatibility of the system [11-14].

* Corresponding author
E-mail address:abdelhakim.zeghoudi@univ-sba.dz

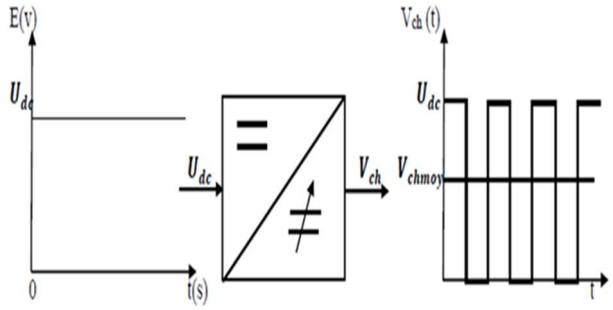

Figure 1. Basic principle of a Chopper.

When studying the radiation of an electromagnetic source, the concept of the radiated field is introduced. When analyzing the radiation of the electromagnetic field, two regions are distinguished: the near-field zone and the far-field zone [15-16].

Near-field scanning (NFS) techniques, as per the guidelines outlined in IEC 61967-3, have gained widespread recognition and extensive industrial applications for effective electromagnetic compatibility (EMC) design and control [13, 17]. These techniques involve the precise placement of one or more field probes in close proximity to the device under test (DUT) and their systematic movement across a defined surface (2D) positioned above the tested object. To capture the radiated near field, either a spectrum analyzer (SA) or a vector network analyzer (VNA) is used in the frequency domain, or an oscilloscope is employed in the time domain**.** Utilizing these methods, valuable information regarding electromagnetic emissions can be obtained, enabling compliance with EMC standards and facilitating efficient design and performance optimization [12-14], [18-21].

Recent studies on electromagnetic interference (EMI) in high-frequency DC-DC converters highlight the importance of characterizing near-field emissions. Zhang et al. showed that power cables significantly influence radiated emissions in an isolated converter[22]. Lai et al. revealed that near-field emissions strongly depend on the switching frequency and circuit geometry[23]. Finally, Boyer et al. proposed a method to predict common-mode conducted emissions from near-field mapping, facilitating the design of electromagnetically compatible systems[24]. Yang et al. modeled near-field emissions of converters based on a monopole antenna, allowing prediction of low-frequency radiation[25]. Lai et al. studied radiated emissions from inductors in electric vehicle converters, proposing a predictive model[26].

The objective of this work is primarily to analyze the radiated electric emissions in the DC/DC converter, particularly in the following electronic components: the IR2110 driver, the IRF740 MOSFET, and the MUR460 diode**.** The rest of this paper is organized as follows: Section 2 describes the electrical diagram of the converter, followed by the PCB implementation, and presents the measurement technique for the near E-field in the components of the series chopper at various MOSFET switching frequencies and duty cycles. In Section 3 presents and discusses the results of the near electric field measurements for all the components mentioned above, focusing on the IR2110 driver and its variation with the control frequency. Section 4 shows the electric field at points A and B, located beneath the diode and the MOSFET, as a function of frequency variation and duty cycle to analyze the obtained results. Finally, Section 5 presents the main conclusions of this work

2. Methodology

2.1 Experimental Setup

Figure 2 shows the electrical diagram in LTspice software, which consists of the following elements: the IR2110 driver, the IRF740 MOSFET, the MUR460 diode, and the 5V and 12V regulators**.** The serial chopper supplied by a DC source of value 20 V and The series chopper is supplied by a 20V DC source, and its square-wave control signal is generated by the Arduino board. The load is a 1.2 kΩ resistor.

Figure 3 shows a photograph of the experimental setup for measuring the near electric field in a series chopper, which consists of the following equipment: a spectrum analyzer and a Rohde & Schwarz electric

probe to measure and visualize the electric field, an oscilloscope to display the MOSFET control signal generated by the Arduino board, and a chopper powered by a DC source**.**

Figure 4 presents a descriptive diagram of the near electric field measurement technique around the Buck converter, focusing on the diode, the MOSFET, and the IR2110 driver, with one analysis based on frequency variation and the other on duty cycle variation**.**

MOSFET or other switch is used in a DC/DC converter, rapid switching creates voltage variations in the circuit. These voltage variations generate a dynamic electric field. Assuming that the voltage variation V(t) is localized, the component of the electric field due to this variation can be approximated by :

$$E(t) = \frac{dv(t)}{dt}\frac{1}{d}$$

Where:

dV(t) is the variation in voltage V(t) over a time interval dt due to switching,

d is the distance between the elements of the circuit where the field is measured.

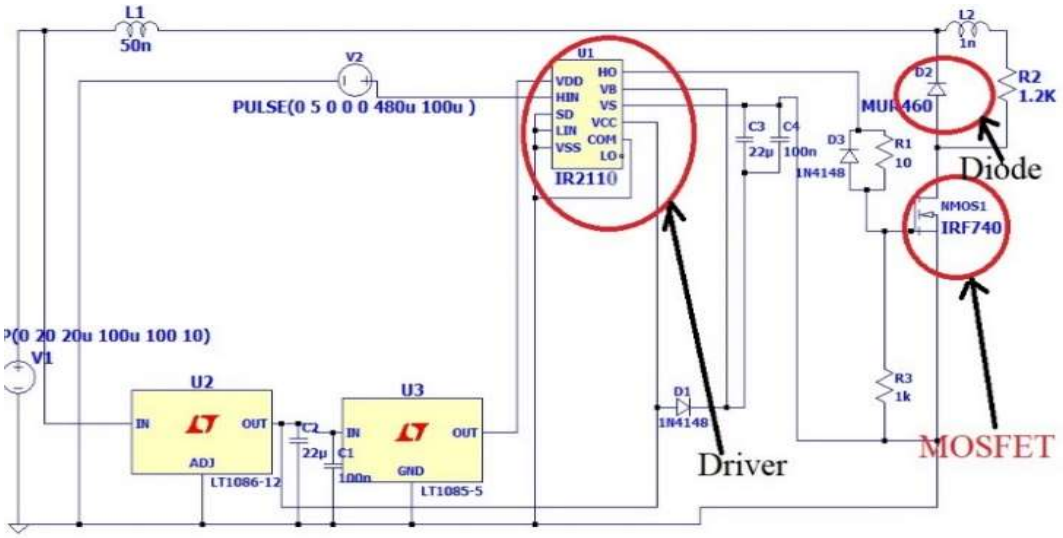

Figure 2. Diagram of serial chopper under Ltspice software.

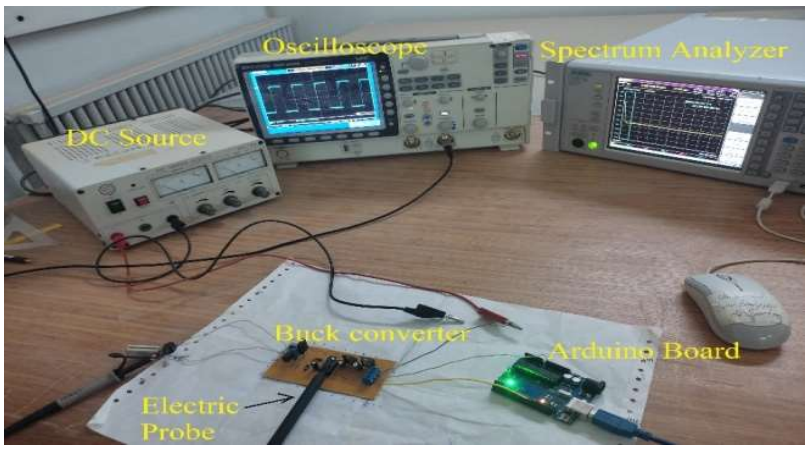

Figure 3. photograph of the near electric field measuring bench.

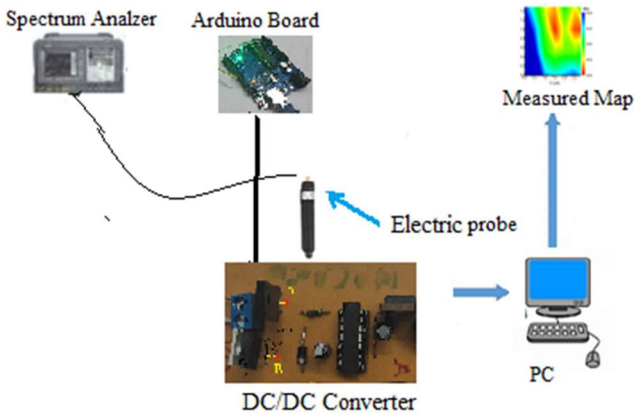

Figure 4. Descriptive diagram of the E-Field measuring bench.

2.2 Measurement Procedure

Figure 5 shows the positions of the E-Field measurement points using the RSE10 electric probe above the series chopper, specifically at point A (x = 0.5 cm, centered on the diode), point B (x = 0.5 cm, centered on the MOSFET), and at the center of the IR2110 driver.

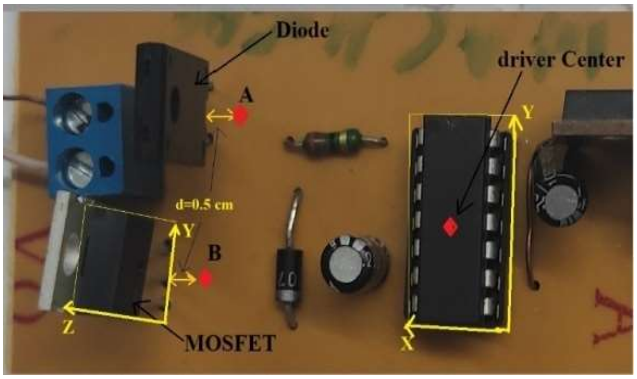

Figure 5. Position of the measurement points of the nearby electric field in the Buck converter.

2.3 Frequency and Duty Cycle Variation

Table 1 presents the control signal frequencies of the MOSFET generated by the Arduino board**.** The selected frequencies are 145.3 kHz, 10 kHz, and 5 kHz, with the following duty cycles: 75%, 50%, and 25%. The signal waveform used is a square wave**.**

Table 1. Different duty cycles and frequencies generated by the Arduino board.

Frequency (kHz)	Duty cycle (%)
5	75
	50
	25
10	75
	50
	25
145.3	75
	50
	25

The APELEC laboratory is equipped with two types of electric field probes manufactured by Rohde & Schwarz: (1) RSE02 and (2) RSE10. These probes are depicted in Figure 6.

2.4 Measurement Points Selection

The RSE02 probe is designed to detect E-fields emitted by bus structures, large components, or power supply structures**.** These fields can potentially cause electromagnetic interference (EMI). The RSE02 probe has a detection area on its bottom surface, measuring approximately 2 cm × 5 cm, as shown in Figure 6**.**

The RSE10 probe, on the other hand, is equipped with a narrow electrode, allowing the selection of a single conductive track from a bundle of tracks that are only 0.2 mm wide. This capability is illustrated in Figure 11. The light-colored probe tip provides a noticeable contrast with the dark green PCB (printed circuit board) [22]**.**

Figure 6. Probes of type ROHDE SHWARZ, probe (1) RSE 02, and probe (2) RSE-10.

The electric field is measured in three components (Ex, Ey, and Ez), as shown in Figure 7, all of which must be considered**.** Dipole probes are used to measure the electric field. These probes are specifically designed to measure a single component of the electric field. The orientation of the dipole determines the direction of the measured electric field**.**

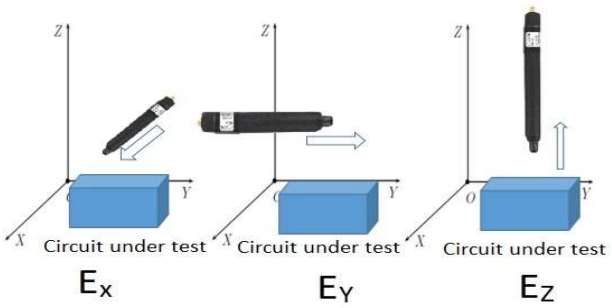

Figure 7. Design and positioning of near field probes for the measurement of all components.

3. Results and Discussion

3.1 Influence of Frequency on EMI

A. Nearby Electric Field above IR2110 Driver

Figure 8 shows the near electric field close to the whole component at z = 0 cm at the center of driver IR2110 for the frequency f = 145.3 kHz, and the duty cycle is 50 %. A greater field is observed in the components E_Z and EX compared to E_Y at -65 dBm for frequency f = 50 MHz, with a subsequent reduction towards the frequency f = 100 MHz.

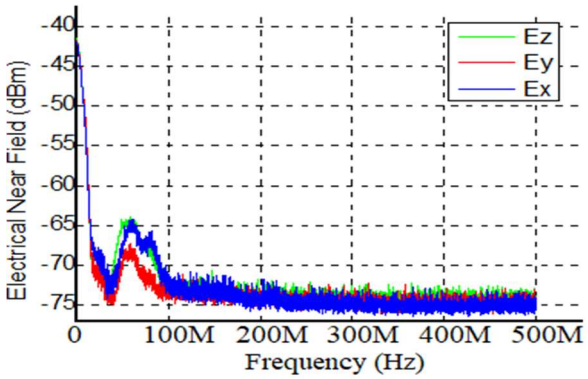

Figure 8. Measured E-Field of all components at z = 0 cm at the center of the driver for the frequency f = 145.3 kHz, and the duty cycle 50%.

Figure 9 shows the electrical emissions as a function of the variation in amplitude z above the driver center for a frequency of f = 145.3 kHz**.** It is observed that with the increase in distance between the driver and the electric probe, the electric field reduces. For the component $E_{Y,}$ A very weak reduction is observed a very slight reduction with the increase in amplitude z, as shown in Figure 10**.**

Figure 11 shows the electric field E_Z as function of the variation in amplitude above the center of Driver IR2110. It is noted that the measured electric field is greater than that of the other components. Additionally, we observe a reduction in electrical emissions as the distance from the measurement point increases.

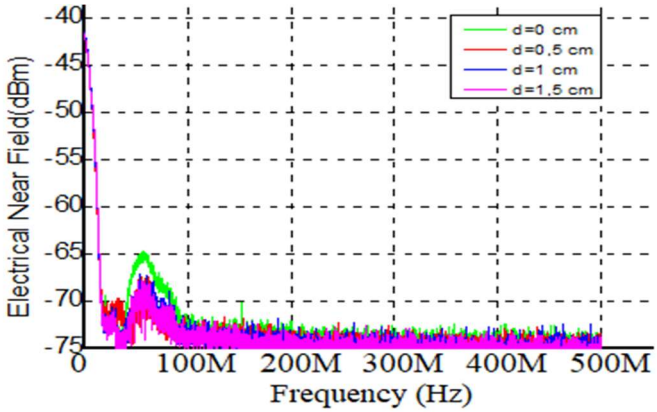

Figure 9. E-Field E_X as a function of the distance above The driver center for the frequency f = 145.3 kHz and duty cycle of 50%

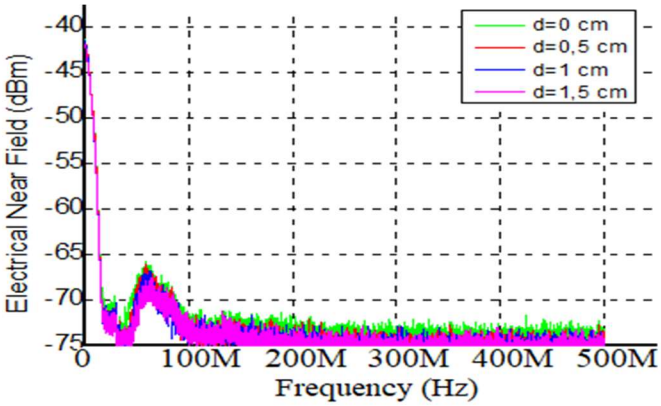

Figure 10. E-Field E_y as a function of the distance above the driver center for The frequency f = 145.3 kHz and duty cycle of 50% .

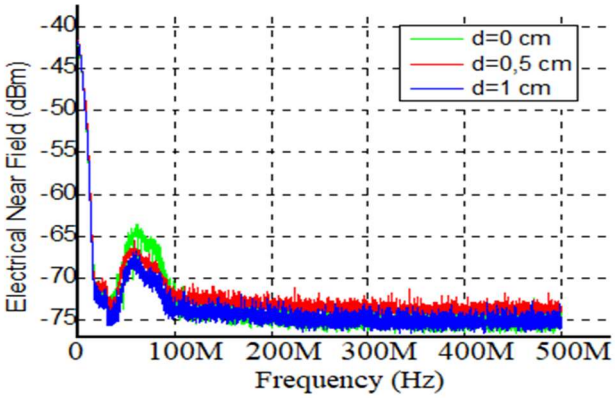

Figure 11. E-Field E_Z as function of the distance above the driver center for the frequency f=145,3 KHz and duty cycle of 50 %.

Figure 12 shows the EZ component of the electric field as a function of the variation in the MOSFET switching frequency, where radiated emissions increase with frequency, starting from about 50 MHz. However, beyond this point, emissions weaken**.**

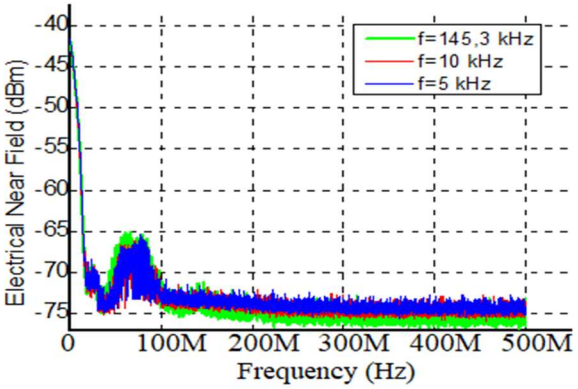

Figure 12. E-Field E_Z as function of the variation of the frequency of MOSFET control at z= 0 cm at the center of the driver.

In this part, the nearby electric field of the component E_Z on the surface of Driver IR2110 was measured by RSE02 probe as shown in Figure 13.

Figure 14 presents the electrical emissions E_z measured by the probe RSE02 according to the variation of the frequency of the switching of the MOSFET to z = 0.5 cm above the driver IR2110. It is observed that the radiated emissions are significant and exceed the CISPR 11 standard limit, followed by a reduction at higher frequencies.

Figure 13. Nearby electric field measurement on the IR2110 driver surface.

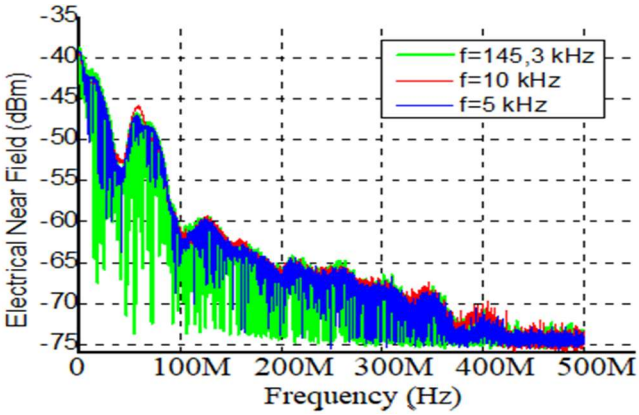

Fig 14. E_Z field measured by the RSE02 probe as Function of the variation of the MOSFET control Frequency at z= 0.5 cm above the driver surface.

Figure 15 shows the impact of varying the duty cycle of the MOSFET switching frequency at z = 0.5 cm**.** No variation in the radiated emissions is noted in relation to the variation of the ratio, while a reduction is observed towards the higher frequencies.

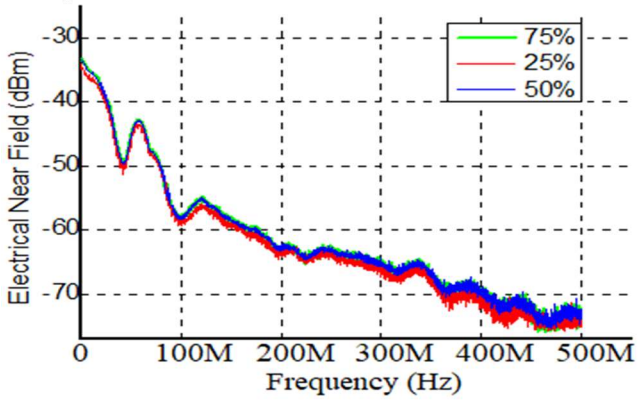

Figure 15. E_Z field measured by the probe RSE02 as fucntion of the variation of the duty cycle f=145.3 at d = 0.5 cm above the driver surface.

Figure 16 shows the impact of variation of the amplitude between the driver IR2110 and the electric probe RSE02. it is observed that as the distance increases, the electric field decreases. This can be explained by the distribution of flux lines in the air**.**

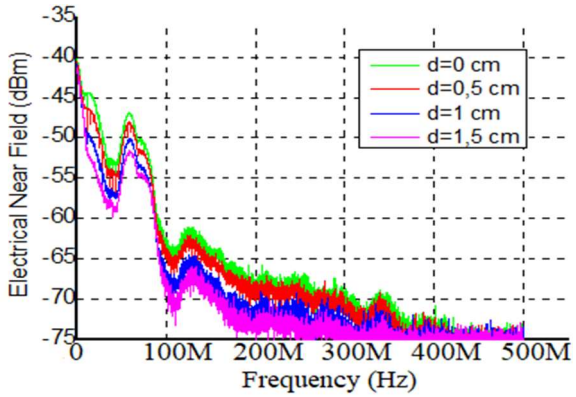

Figure 16. E_Z field measured as function of the variation of the distance above the driver surface for the frequency f = 145.3 kHz and duty cycle 50%

B. E-Field above the Diode

The measurement of the electric field for all components around the diode type MUR460 was initiated. The impact of distance variation and the frequency variation of the control signal in the chopper series were analyzed. Next, the impact of variation of the duty cycle is studied. Figure 17 presents the electric field measured by the probe RSE10 of all the components for the frequency f = 145. 3 kHz, and the duty cycle is equal to 50%. It is observed that the electric field is very low. However, the EZ component is stronger than the EY and EX components at 50 MHz (-65 dBm), followed by a rapid decrease towards 100 MHz. Beyond this frequency range, the electric field is negligible.

Figures 18, 19 and 20 show the electric field of all components E_X, E_Y, E_Z respectively as function of the variation of the distance between the measuring point and the diode terminals in the *X* direction. It is noted that as the measuring point increases, the electric field decreases. However, this reduction is minimal due to the small surface area of the measuring dipole. A further reduction occurs towards 100 MHz, and beyond this frequency, the electric field is negligible**.**

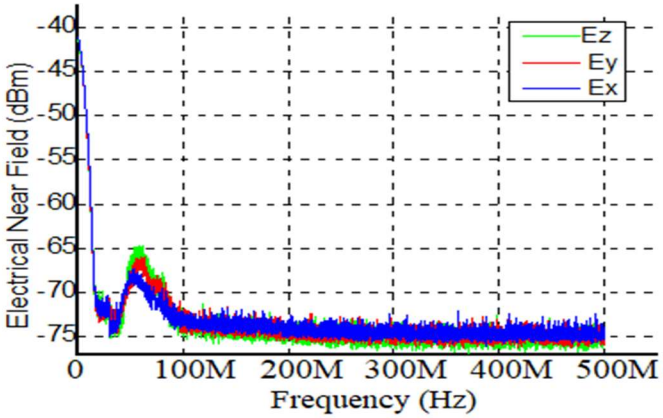

Figure 17. electric field of all components measured by the probe RSE10, at point A for the Frequency f=145.3 KHz, and Duty cycle 50%.

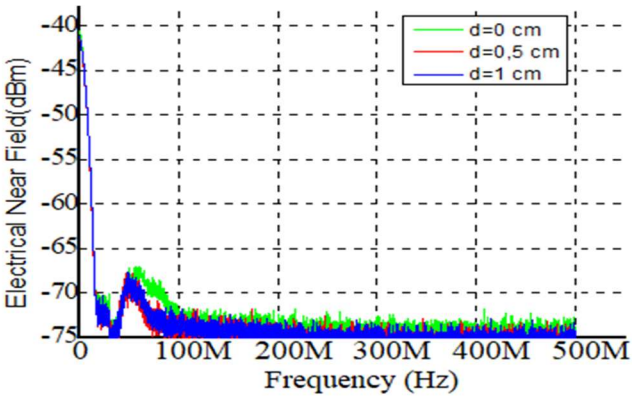

Figure 18. E_X field as function of the variation of the distance to the diode at point A for the frequency f = 145.3 kHz.

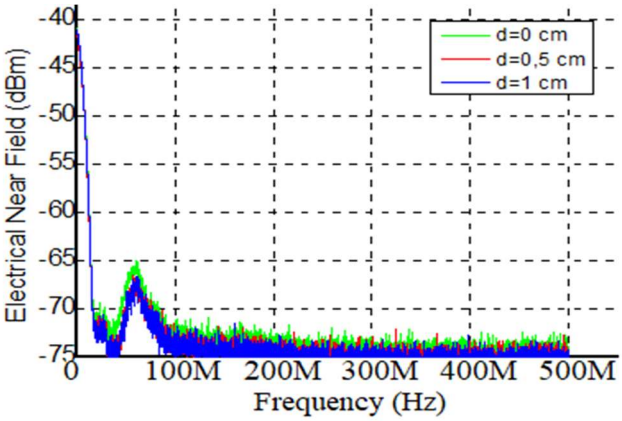

Figure 19. E_y field as function of the variation of the distance to the diode at point A forthe frequency f = 145.3 kHz.

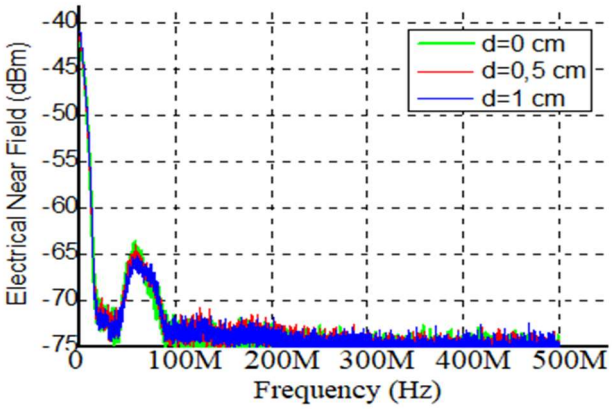

Figure 20. E_z field as function of the variation of the distance to the diode at point A for the frequency f = 145.3 kHz.

Figure 21 presents the electric field E_Z as function of the variation of the control frequency of the MOSFET at point A. A peak in the radiated emissions is observed, exceeding -65 dBm at the frequency f = 145.3 kHz. followed by an alignment between the three cases beyond 100 MHz

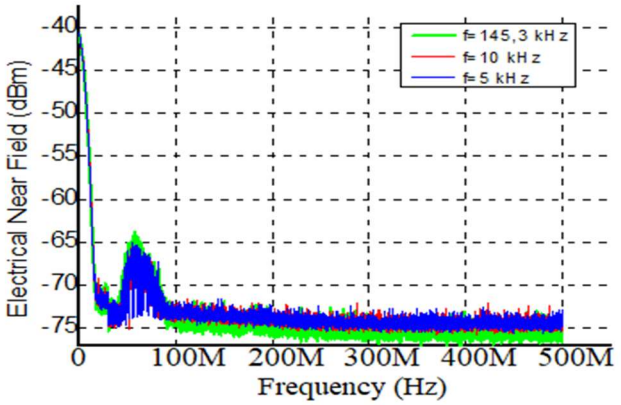

Figure 21. E_Z field as function of the variation of the MOSFET control frequency at point A.

Figure 22 presents the electrical emissions measured by the probe RSE02 at the surface of diode and MOSFET in the direction *X* at *x* = 0 cm between the electric probe and the diode. The near electric field measured presents the field emitted by the diode and the MOSFET, and the output of series chopper.

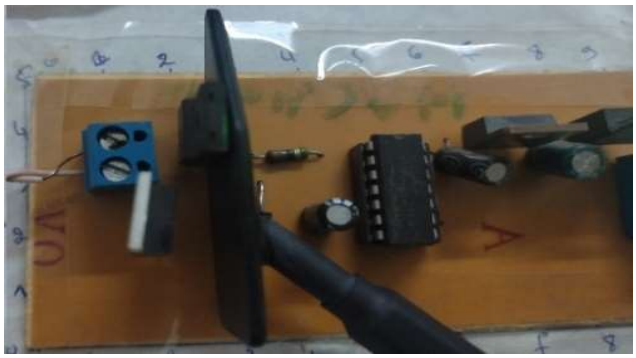

Figure 22. Position of the measuring probe RSE02 in the X direction.

Figure 23 shows E_Z field as function of the variation in distance between the RSE02 probe and the diode in the *X* direction for the frequency f = 145.3 kHz, where it is clearly seen with increasing distance, the electric field reduces. So, the electric noise exceeds the limit of CISPR 11 class A. Next, a reduction at higher frequencies**.**

Figure 24 shows the electric field at $d = 0$ cm in the *X* direction as function of the variation of the switching frequency of the MOSFET. It is noticed that a peak in electric noise at 50 MHz exceeding -40 dBm, followed by a reduction at higher frequencies, with oscillations observed between 200 MHz and 500 MHz**.**

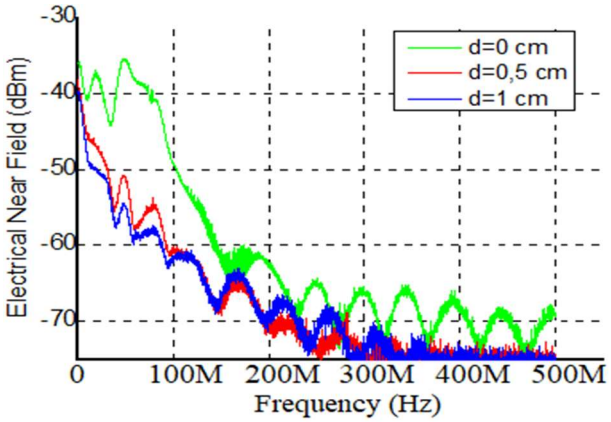

Figure 23. E-Field E_Z as function of the variation of the distance X to the diode and MOSFET for the frequency f = 145.3 kHz.

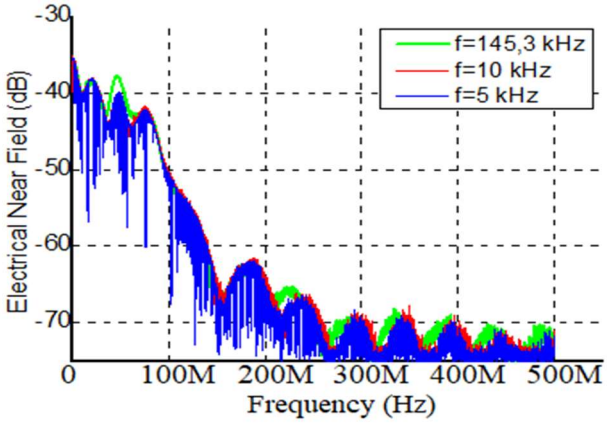

Figure 24. E-Field E_Z as function of the variation of the switching frequency of the serie chopper at x=0 cm with respect to the diode and MOSFET

C. Near Electric Field above the MOSFET

In the second part, the electric field emitted by the MOSFET terminals at point B was measured across all components. Figure 25 illustrates the electric field measured by the RSE10 probe at point B for the frequency f = 145.3 kHz, with a duty cycle of 50%. It is observed that the maximum of the EX component exceeds the other components at f = 50 MHz, attributed to the terminals being oriented in the X direction, followed by a reduction towards 100 MHz.

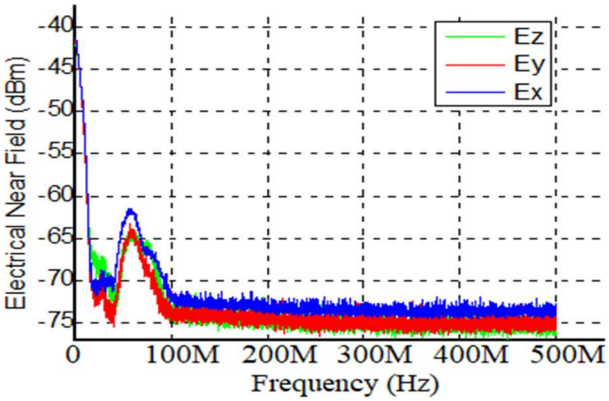

Figure 25. Electric field of all the components measured by the RSE10 probe, at point B for the frequency f= 145.3 KHz, and duty cycle 50%.

Figures 26, 27 and 28 present the impact of variation the distance between the point of measurement and the center of MOSFET type IRF740 on the near electric field for f = 145.3 kHz in all components E_X, E_Y and E_Z respectively. It is observed that the electric field is very weak due to the small surface area of the measurement dipole, making the impact of field variation with distance minimal.

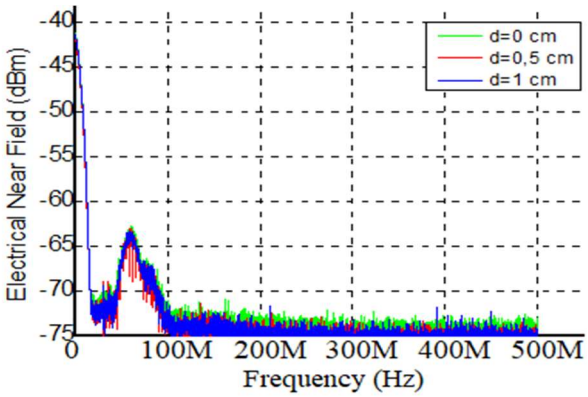

Figure 26. E_X field as function of the variation of the distance to the MOSFET at point B for the frequency f = 145.3 kHz.

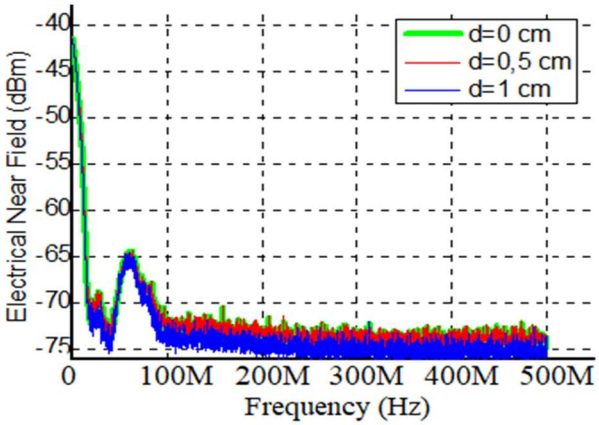

Fig 27. E_y field as function of the variation of the distance to the MOSFET at point B for the f = 145.3 kHz.

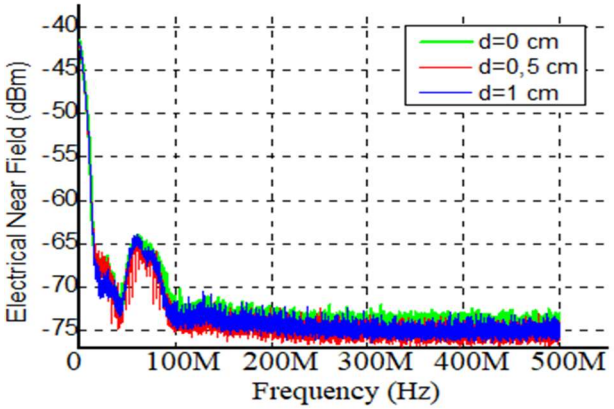

Figure 28. E_z field as function of the variation of the distance to the MOSFET at point B for the frequency f = 145.3 kHz.

Figure 29 presents the electric field at the point B according to the variation of the frequency of commutation. We notice that the near electric field measured in the MOSFET at d = 0.5 cm by the probe RSE10, and in the diode at d = 0.5 cm (Fig. 21) almost identical. So, A peak in the radiated emissions is noted, exceeding -67 dBm at the frequency f = 50 MHz. These emissions increase with frequency, then rapidly decrease up to 100 MHz, after which the electric field becomes insignificant.

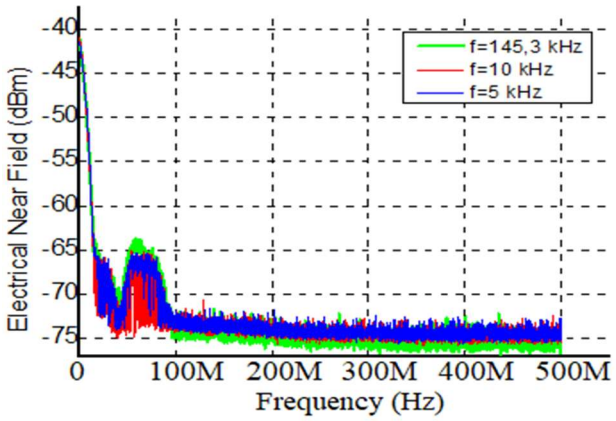

Fig 29. E_X field as function of the frequency variation of the signal at point B.

From the obtained results, it can be concluded that the near electric field depends on the variation in distance between the measurement point and the circuit under test. The measured components (X, Y, and Z) are

influenced by the MOSFET switching frequency variation, duty cycle, and the measurement dipole surface area**.**

4 Conclusion

In this study, A method for measuring the near electric field was explored using available probes in the frequency domain, specifically employing a spectrum analyzer along with the serial chopper. The study focused on electronic components such as the IR2110 driver, IRF740 MOSFET, and diode, examining their behavior in relation to distance variation and the switching frequency of the MOSFET. Additionally, the impact of varying the duty cycle on the electric probes available in the laboratory was analyzed. The findings reveal that probes with larger surface areas capture a more significant field compared to those with smaller surface areas.

acknowledgment

The authors express their gratitude to the General Directorate of Scientific Research and Technological Development (DGRSDT) in Algeria for their valuable technical support and for providing the dedicated research budget for this program.

References

[1] S. Dimitar, L.Vladimir, "Modeling of static dc-dc converters for renewable energy applications using matlab/silink ", Université Technique de Sofia, 8 Kliment Ohridski, Sofia 1000, Bulgarie, Conférence EF 2009 UTC, Compiègne, 24-25 (Septembre 2009).

[2] G. Frantz, "System approach for the study of the electromagnetic compatibility of on-board networks ", Thesis, Energieélectrique. Université Grenoble Alpes, (2015).

[3] Zeghoudi , A. Bendaoud , H. Slimani, H. Miloudi, M. Miloudi, N. Chikhi, ”Experimental Measurement of Common and Differential Modes for Variable Speed Drive DC Motor”, IEEE multiconference on Signal, System, Devices (SSD), Setif, Algeria, (2022), DOI: 10.1109/SSD54932.2022.9955933.

[4] R. Pinill, "Design of electronic power converters with low electromagnetic impact integrating new technologies of semiconductor switches", Thesis, université de Lyon, (2014).

[5] H. Slimani, A. Zeghoudi, A Bendaoud, A. Reguig, B. Benazza, N. Benhadda, ”Experimental Measurement of Conducted Emissions Generated by Static Converters in Common and Differential Modes”. European Journal of Electrical Engineering (EJEE) 23 (June 2019): 273–279, 2021. DOI:10.18280/ ejee.230312 .

[6] Zeghoudi, A. Bendaoud, H. Slimani, B. Benazza and Bennouna Determination of electromagnetic disturbances in a buck chopper, Australian Journal of Electrical and Electronics Engineering, (2022), DOI: 10.1080/1448837X.2021.2023073.

[7] Benhadda N., Bendaoud A., Chikhi N. , “A conducted EMI noise prediction in DC/DC converter using a frequency-domain approach“, ElektrotehniškiVestnik Journal 85(3): 103-108, (2018).

[8] Zeghoudi, A. Bendaoud, S. Khalladi, H. Slimani, H. Miloudi, L. Canale, “Common And Differential Modes Filter For The PFC Boost AC/DC LED Driver , 22nd International conference on environment and electrical engineering, 6th Industrial and commercial power systems Europe Prague, Czech Republic June 28th - july 1st, (2022),

[9] doi:10.1109/EEEIC/ICPSEurope54979.2022.9854760

[10] Zeghoudi, A. Bendaoud, L. Canale, A. Tilmatine and H. Slimani, "Common Mode and Differential Mode noise of AC/DC LED Driver," 2021 IEEE International Conference on Environment and Electrical Engineering and 2021 IEEE Industrial and Commercial Power Systems Europe (EEEIC / I&CPS Europe), pp.1-6, (2021)doi: 10.1109/EEEIC/ICPSEurope51590.2021.9584616.

[11] Moreau M., "High frequency modeling of energy converters. Application to the study of emissions conducted to the network ", PHD Thesis, Electrical Engineering, Central School of Lille-France, (2009).

[12] Zeghoudi, H. Slimani, A. Bendaoud, B. Benazza, S. Bechekir, H. Miloudi. Measurement and analysis of common and differential modes conducted emissions generated by an AC/DC converter.

Electrical engineering & electromechanics, (2022), no.1, pp. 3-9. doi: 10.20998/2074-272X.2022.1.01.

[13] A. Zeghoudi, A. Bendaoud, H. Slimani, H. Miloudi, M . Miloudi, L. Canale, "Exprimental Measurement of Near Magnetic Field by different probe for AC/DC LED Driver , 22nd International conference on environment and electrical engineering, 6th Industrial and commercial power systems Europe Prague, Czech Republic June 28th - july 1st, (2022), doi:10.1109/EEEIC/ICPSEurope54979.2022.9854788

[14] Y. Lai, J. Yao , S. Wang , Z. luo, Y. Li "Electric Near Field Emission From a 1Mhz Power Converter For Electric Vehicles "2021 IEEE Energy Conversion Congress and Exposition (ECCE), Vancouver, BC, Canada, , (November 2021),DOI: 10.1109/ECCE47101.2021.9595815.

[15] X. Wu, F. Grassi , S. A. Pignari , U. Paoletti, I. Hoda, "Performance of Electric Near-Field Probes for Immunity Tests" 2020 XXXIIIrd General Assembly and Scientific Symposium of the International Union of Radio Science , Rome, Italy, (oct 2020), DOI:10.23919/URSIGASS49373.2020.9232438.

[16] S. Akue Boulingui, "Study of the electromagnetic coupling between integrated circuits by emulation of the disturber - Application in 3G telephony", Thesis, Toulouse, France, (2009).

[17] J. C. Bolomey, F. E. Gardiol, "Engineering applications of the modulated scatterer technique", Artech House, (2001).

[18] A.Ramanujan, "Development of automated frequency and time-domain radiated electromagnetic emission models for microelectronic applications," PhD dissertation, Univ. of Rouen, (2011).

[19] B. Essakhi, D. Baudry, O. Maurice, A. Louis, L. Pichon, and B. Mazari, "Characterization of radiated emissions from powerelectronic devices: Synthesis of an equivalentmodel from near-field measurement," *Eur. Phys. J. Appl. Phys.*, vol. 38, pp. 275–281, (2007).

[20] S. Saidi and J. Ben HadjSlama, "A near-field technique based on PZMI, GA, and ANN: Application to power electronics systems," *IEEE Trans. Electromagn. Compat.*, vol. 56, no. 4, pp. 784–791, (Aug. 2014), DOI: 10.1109/TEMC.2013.2290271.

[21] A. Zeghoudi, A. Bendaoud, A. Tilmatine, S. Bechkir, G Zissis, L. Canale, "Study of the impact of the power dimming and lighting modes of LED lamps on the near magnetic field", Optik, Volume 271, 2022, 169997, ISSN 0030-4026, https://doi.org/10.1016/j.ijleo.2022.169997.

[22] Baudry, C. Arcambal, A. Louis, B. Mazari, and P. Eudeline, 'Applications of the Near- Field Techniques in EMC Investigations', IEEE Transactions on Electromagnetic Compatibility, vol. 49, no. 3, August (2007), DOI:10.119/TEMC/.2007.902194.

[23] R&S®HZ-15/R&S®HZ-17 Probe Sets R&S®HZ-16 Preamplifier " E and H near-field emission measurements with test receivers, spectrum analyzers and oscilloscopes "Broduct Brochure version 01.00

[24] Y. Zhang, S. Wang and Y. Chu, "Investigation of Radiated Electromagnetic Interference for an Isolated High-Frequency DC–DC Power Converter With Power Cables," in *IEEE Transactions on Power Electronics*, vol. 34, no. 10, pp. 9632-9643, Oct. 2019, doi: 10.1109/TPEL.2019.2892706

[25] YY. Lai, J. Yao, S. Wang, Z. Luo and Y. Li, "Electric Near Field Emission From a 1Mhz Power Converter For Electric Vehicles," *2021 IEEE Energy Conversion Congress and Exposition (ECCE)*, Vancouver, BC, Canada, 2021, pp. 2881-2887, doi: 10.1109/ECCE47101.2021.9595815.

[26] Boyer, N. Nolhier, F. Caignet and S. B. Dhia, "Anticipating Common-Mode Conducted Emission of DC-DC Converter from Electric Near-Field Scan," *2021 IEEE International Joint EMC/SI/PI and EMC Europe Symposium*, Raleigh, NC, USA, 2021, pp. 603-608, doi: 10.1109/EMC/SI/PI/EMCEurope52599.2021.9559364.

[27] Y. Yang, Y. Lai, S. Wang and Z. Luo, "Modeling and Prediction of Low-Frequency Near-Field Radiation for a Power Converter Based on the Operating Principle of a Monopole Antenna," in *IEEE Transactions on Power Electronics*, vol. 39, no. 11, pp. 14387-14397, Nov. 2024, doi: 10.1109/TPEL.2024.3441810

[28] Y. Lai, Y. Yang, S. Wang and Z. Luo, "Modeling of Low-frequency Radiated EMI from the Inductors of Power Converters in Electric Vehicles," in *IEEE Transactions on Transportation Electrification*, doi: 10.1109/TTE.2024.3519259.